ACS OMEGA

Article

http://pubs.acs.org/journal/acsodf

Assembly of Organosolv Lignin Residues into Submicron Spheres: The Effects of Granulating in Ethanol/Water Mixtures and Homogenization

Xin Rao, Yongzhuang Liu, Qi Zhang, Wenshuai Chen, Yixing Liu, and Haipeng Yu*

Key Laboratory of Bio-Based Material Science and Technology of Ministry of Education, Northeast Forestry University, Harbin 150040, P. R. China

Supporting Information

ABSTRACT: The production of chemicals and various materials from black liquor lignin will greatly improve the economics of biomass refining. In the present work, organosolv lignin residues (OLRs) from the organosolv pulping process were used to fabricate submicron lignin spheres using ethanol/water mixtures as an antisolvent, in conjunction with homogenization. Both the ethanol content in the ethanol/water mixture and the applications of homogenization were investigated as key factors affecting the agglomeration of OLRs. The results show that the solubility of the amphiphilic OLRs in ethanol was approximately 28 and 32 times greater than those of alkali lignin and kraft lignin, respectively. Using the optimal percentage of ethanol together with homogenization enhanced the nucleation of lignin macromolecules, such that the colloidal spheres of OLR were spontaneously assembled via gradual hydrophilic−lipophilic aggregation. The resulting OLR colloidal spheres had a yolk−shell structure and a mean particle diameter of around 200 nm, when the ethanol content was 50% and the homogenization time was 15 min or more. This study demonstrates a simple means of utilizing OLRs to produce lignin-based spheres. The lignin spheres generated in this work are thought to have potential applications in many fields as porous carbon precursors for energy storage, sensitive functional materials, and controlled-release fertilizer carriers.

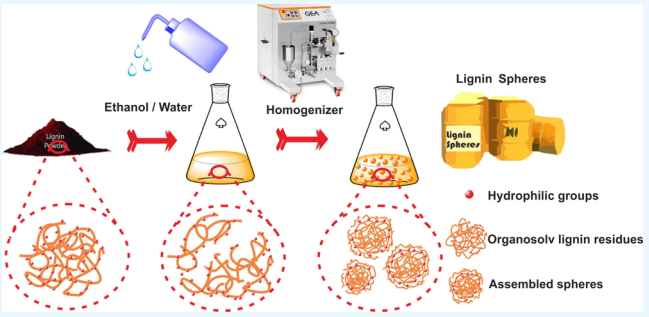

INTRODUCTION

Lignin is an important component of plant cell walls and the most abundant aromatic polymer in nature, accounting for 10−35% of biomass by weight and up to 40% on an energy basis.[1,2] However, most current processes that generate lignin consider this to be a material part of the waste stream. Only a small percentage of lignin is used in commercial applications, such as a low-grade fuel, an additive for pitch, a modification filler in rubber, and a culture medium for the plant tissue.[3−5] Kraft lignin and alkali lignin are typical industrial lignin products that primarily originate from the black liquor produced by pulping.[6] Approximately, 7 tonnes of black liquor are produced to obtain 1 tonne of pulp. Kraft lignin and alkali lignin have been used for energy production or commercially applied as additives, binders, dispersants, and surfactants.[7−10] However, the transformation of these industrial lignin products to value-added materials using a simple process would be extremely beneficial. Therefore, an efficient and high value-added approach to utilizing lignin is highly desirable.

Recently, various researchers have reported the preparation of nanolignin, colloidal nanospheres, or nanocapsules from kraft or alkaline lignin, based on the reactions of functional groups, through facile mechanical or chemical mechanisms.[11−18] Nair et al. reported that lignin nanoparticles were obtained from kraft lignin by high shear homogenization and subsequently used to improve the thermal stability of lignin/poly(vinyl alcohol) blends.[11] Lignin nanoparticles were also produced by Gilca et al. by sonication of the commercial wheat and grass lignin.[15] Nevertheless, the lignin nanoparticles synthesized by mechanical processing generally have irregular shapes. On account of this issue, Lievonen et al. developed a simple means of making kraft lignin nanospheres based on introducing water to a tetrahydrofuran (THF) phase followed by dialysis.[16] Li et al. also produced lignin nanospheres merely by mixing a kraft lignin/ethanol solution with water and demonstrated that the ethanol concentration has a significant effect on the assembly of the nanocapsules.[19] These advances have demonstrated new applications of black liquor lignin and have also challenged the conventional understanding of lignin morphology.

On the basis of the above studies, it is apparent that solvents can play an important role in the formation of nanosphere or nanocapsule structures. However, the poor solubility of kraft lignin in organic solvents limits the yield of such processes. For this reason, chemical modifications such as acetylation, grafting, and cross-linking have been applied to improve the solubility or

Received: March 10, 2017
Accepted: June 7, 2017
Published: June 21, 2017

DOI: 10.1021/acsomega.7b00285
ACS Omega 2017, 2, 2858−2865

to insert functional groups for further assembly, although such processes are often environmentally unfriendly.[13,14] Thus, there is a need to identify an ideal feedstock that exhibits good solubility in organic solvents without modification. This material should also exhibit more reactive moieties in organic solvents and should be directly used as the raw material for various nanostructures without any modification.

With the development of organosolv pulping for biorefinery, the utilization of whole products, especially the by-products, has a crucial meaning on the environment. The main by-product of the organosolv biorefinery of biomass is organosolv lignin that is generated in large quantities by the organosolv pulping process.[20] In this process, organic solvents are used to fractionate the lignin at elevated temperatures, leaving behind holocellulose residues. To the best of our knowledge, the utilization of organosolv lignin as building blocks for the assembly of lignin nanostructures has not been studied in detail. In particular, the effect of the combination of solvent and mechanical working on the formation of organosolv lignin-based nanostructures has not yet been reported.

In the present study, the organosolv lignin residue (OLR) that is separated from the alcohol-based black liquor was used as a feedstock. The chemical structure of the OLR was subsequently characterized using a two-dimensional hetero-nuclear single quantum coherence nuclear magnetic resonance (2D HSQC NMR) spectroscopy, Fourier transform infrared (FTIR) spectroscopy, and ultraviolet−visible (UV−vis) spectroscopy. The molecular weight of the OLR was also determined by using gel permeation chromatography (GPC). In addition, the submicron lignin spheres were fabricated by dispersing the OLR in ethanol/water mixtures followed by homogenization. This work examined both the effects of the ethanol content in the solvent mixture and the use of homogenization on the formation of OLR-based colloidal spheres. Transmission electron microscope (TEM) and atomic force microscope (AFM) were used to observe the morphology of the spheres.

RESULTS AND DISCUSSION

The yield of Klason lignin purified from OLR was 14.71%, representing 73.44% of the total lignin (20.03%) in the raw wood (Table 1). This was due to the dissolution of partial lignin components during the extraction process. The lignin fractionation result was nearly equal to that (15.53%) reported from an acidified sodium chlorite process.[21] The structural variations of the OLR were characterized using a 2D HSQC NMR spectroscope. As shown in Figure 1, the primary lignin signals appear in the side-chain region (δ_C/δ_H 50−110/2.5−6.0 ppm) and the aromatic region (δ_C/δ_H 100−135/5.5−8.0 ppm). The main cross-signals were assigned according to the literature[22,23] and are listed in Table 2. The cross-signals that are typical of lignin−carbohydrate complex (LCC) structures were not observed in the carbohydrate region (δ_C/δ_H 91−105/3.9−5.4 ppm), and the cross-signals of both benzyl ether and xylans disappeared. This result demonstrates that the primary linkages between xylans and lignins were cleaved by the alcoholysis and that hemicellulose (the primary component of the LCC structure) was dissolved during the alcoholysis process. The liberated lignin was dissolved in ethanol, leading to the fractionation of the wood lignocellulose. In the aromatic regions, both $S_{2/6}$ (δ_C/δ_H 103.8/6.64 ppm) and G_5 (δ_C/δ_H 115.4/6.81 ppm) signals were the primary peaks generated by the poplar wood. The cross-signals demonstrate that the OLR was mainly composed of syringyl (S)- and guaiacyl (G)-type lignin units. Condensed cross-signals were also evident, possibly as a result of the OLR precipitation. In the side-chain region, in addition to the strong methoxyl group signals (δ_C/δ_H 56.1/3.77 ppm), the main signals were attributed to the condensed lignin structures (δ_C/δ_H 60.0/3.69 and 60.5/3.83 ppm), and the signals of β-β' structures and small amounts of typical xylans were also detected. This reveals that the main lignin linkages of β-O-4′ were cleaved with respect to the milled wood lignin (MWL) of the raw wood (Figures S1 and S2). These results demonstrate that the lignin condensation occurred during the precipitation of the OLR. The obtained OLR was rich in carbon-to-carbon bonds, with a small amount of carbohydrates.

Table 1. Yield of Lignin Prepared by Different Methods

methods	lignin/%
organosolv method	14.71
Klason method	20.03
acidified sodium chlorite treatment	15.53

The weight-average (M_w) and the number-average molecular weights (M_n) of the OLR as determined by GPC were 6708 and 3011 g mol^{-1}, respectively, and so, the polydispersity index (PDI) was 2.23. This PDI suggests that the OLR has a narrow particle size distribution. After the homogenization process in 50% ethanol for 45 min, M_w and M_n were slightly decreased to 6672 and 2570 g mol^{-1}. This reveals that the homogenization process affected little on the molecular weights of OLR. Owing to the hydrophobic nature of lignin and the hydrophilic characteristics of carbohydrates, the OLR represents a polymer with amphiphilic properties. This is beneficial with regard to its eventual application as a building block for the assembly of various structures.[24]

When considering the self-assembly of lignin nano- or microstructures, the yield of the product is directly related to the solubility of lignin in the solvent. The solubilities of OLR, kraft lignin, and alkali lignin in ethanol were assessed in this study and were found to be 2.15, 0.066, and 0.077 wt %, respectively. The solubility of OLR was, therefore, approximately 32 and 28 times those of the kraft lignin and alkali lignin. This difference was deemed to result from the degree of fractionation of OLR and to have an impact on its functional groups during the organosolv process.[25] Typically, lignin is extracted by organic solvents owing to the high solubility of this material and is readily recovered by evaporation of the solvent. Thus, the OLR obtained in this study is considered to represent an ideal feedstock for studying the effects of granulating with ethanol/water mixtures, followed by homogenization.

TEM was used to observe the morphology of OLR aggregates resulting from different ethanol/water ratios and the morphologic variations after homogenization. As shown in Figure 2, the OLR in pure water displayed no definite shape (Figure 2a). However, in an aqueous solution with 25% ethanol, the OLR aggregated to form colloidal particles with irregular shapes (Figure 2b). As the ethanol content was increased to 50%, the OLR aggregates transitioned into spheres with sizes in the range of 100−250 nm (Figure 2c). At 75% ethanol, the OLR was present primarily as uniform colloidal spheres with sizes close to 150 nm, except for some zonally interconnected clusters of spheres (Figure 2d). This occurred because, after the addition of ethanol, the hydrophilic moieties

DOI: 10.1021/acsomega.7b00285
ACS Omega 2017, 2, 2858−2865

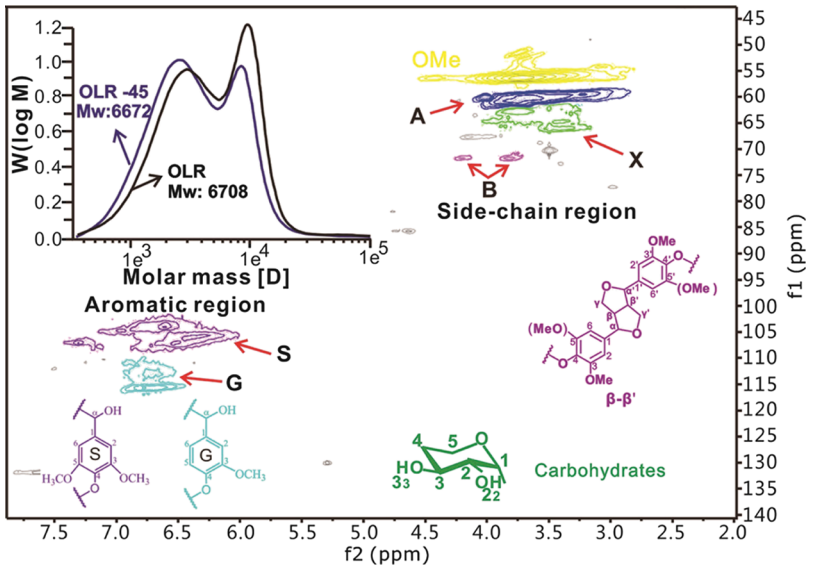

Figure 1. 2D HSQC NMR spectra of the OLR. Inset is the distribution of molecular weights by the GPC analysis. The black line represents the OLR, and the blue line represents the OLR after the homogenization treatment for 45 min.

Table 2. Assignment of $^{13}C-^{1}H$ Cross-Signals in the HSQC Spectra of OLR

	δ_C/δ_H	assignment
C_β	53.62/3.47	$C_\beta-H_\beta$ in phenylcoumarin substructures (C)
B_β	54.15/3.06	$C_\beta-H_\beta$ in resinol substructures (B)
−OMe	56.26/3.74	C−H in methoxyls
A_γ	58.98−60.56/3.40−3.72	$C_\gamma-H_\gamma$in β-O-4′ substructures (A)
A'_γ	63.96/4.37−4.47	$C_\gamma-H_\gamma$ in γ-acylated β-O-4′substructures (A_γ and A′)
B_γ	71.65/3.91 and 4.19	$C_\gamma-H_\gamma$ in resinol substructures (B)
$(A, A_\gamma)_\alpha$	72.52/4.83	$C_\alpha-H_\alpha$ in β-O-4′ substructures (A) and γ-acylated β-O-4′ substructures (A′)
B_α	85.55/4.67	$C_\alpha-H_\alpha$ in resinol substructures (B)
C_α	87.48/5.44	$C_\alpha-H_\alpha$ in phenylcoumaran substructures (C)
X5	60.20/3.40 and 3.73	C_5-H_5 in β-D-xylopyranoside
$S_{2,6}$	103.94/6.68	$C_{2,6}-H_{2,6}$ in etherified syringyl units (S)
$S'_{2,6}$	106.21/7.23 and 7.05	$C_{2,6}-H_{2,6}$ in oxidized (C_α=O) syringyl units (S′)
G_2	111.36/6.95	C_2-H_2 in guaiacyl units (G)
G_5	115.64/6.81	C_5-H_5 in guaiacyl units (G)
G_6	119.67/6.81	C_6-H_6 in guaiacyl units (G)
$PB_{2,6}$	131.84/7.69	$C_{2,6}-H_{2,6}$ in p-hydroxybenzoate substructures (PB)

of OLR had an affinity to ethanol, leaving the hydrophobic portions of the dissociated lignin aggregating together to form the spheres.[13,19,24] However, because the hydrophilic moieties were distributed randomly in the OLR, abundant hydrophilic moieties would expose to ethanol constantly during the homogenization process. Therefore, regular OLR-based spheres were obtained using the optimal percentage of ethanol together with the homogenization process (Figure S3).

Figure 3 presents the morphological differences between the OLR aggregates assembled in a 50% ethanol solution as the homogenization time is varied. The OLR aggregates appeared to be composed of globular clusters but presented no particular morphology before homogenization (Figure 3a). After homogenization for 5 min, the OLR aggregates gradually changed to almost spherical structures with a yolk−shell construction having diameters within the range of 200−300 nm (Figure 3b). Following 15 min of continuous homogenization, independent OLR-based colloidal spheres were found with sizes of approximately 230−250 nm (Figure 3c). Increasing the homogenization time to 45 min generated more spherical OLR-based submicron spheres with sizes within the range of 170−260 nm, but the yolk−shell construction was not apparent yet (Figure 3d). These OLR-based submicron spheres were found to be uniformly distributed based on the AFM images (Figure 4). The above results indicate that both the ethanol content and the homogenization time play important roles in forming the OLR-based submicron spheres. Low ethanol content tends to prevent the formation of a spherical morphology, whereas longer homogenization time promotes the production and the densification of the spheres.

The functional groups of the OLR and the OLR-based spheres were characterized by FTIR analysis (Figure 5). The spectra exhibit a peak at 3410 cm^{-1} that corresponds to hydroxyl groups. Compared with the peak position (3334 cm^{-1}) of wood lignocellulose, the hydroxyl peak of the OLR exhibits a blue shift. This is attributed to the exposure of a greater quantity of phenolic hydroxyl groups in the lignin following the removal of cellulose and hemicellulose.[25] The peak at 2934 cm^{-1} corresponds to the asymmetric stretching vibrations of methoxy, methyl, and methylene groups. The

DOI: 10.1021/acsomega.7b00285
ACS Omega 2017, 2, 2858−2865

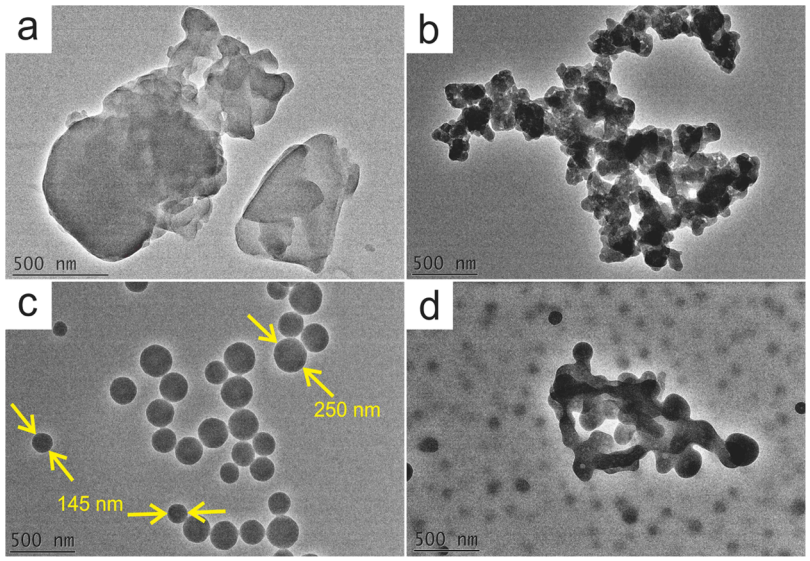

Figure 2. TEM images show the morphological differences of the OLR aggregates in the ethanol/water solution with an ethanol content of (a) 0, (b) 25, (c) 50, and (d) 75%, in conjunction with a homogenization treatment of 15 min.

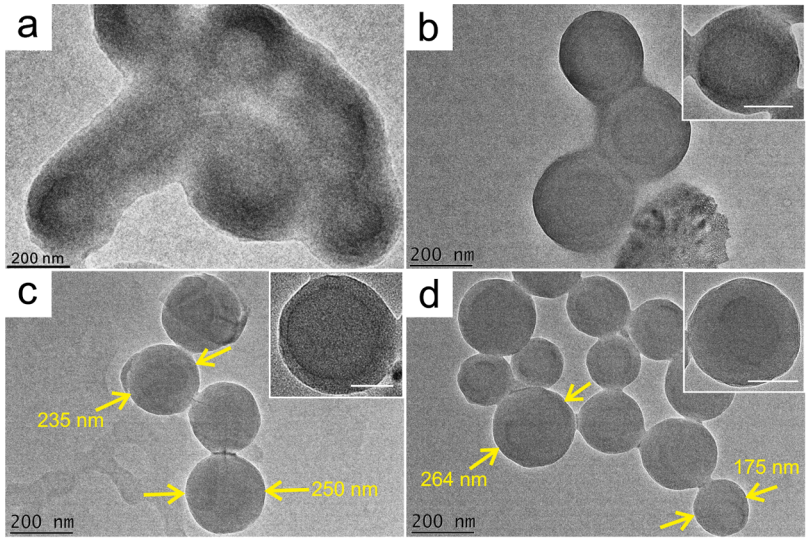

Figure 3. TEM images of the OLR aggregates in the ethanol/water solution (ethanol content: 50%), in conjunction with a homogenization treatment of (a) 0, (b) 5, (c) 15, and (d) 45 min, respectively. The scale bar in the insets is 100 nm.

peaks at 1593 and 1506 cm^{-1} are attributed to the skeletal vibrations of benzene and carbonyl stretching, respectively, and are more intense in the lignin spectra than in the wood spectra. The peaks at 1456 and 1267 cm^{-1} are ascribed to C−H bending and benzene or C═O stretching vibrations and are present in the spectra of OLR but not the wood. The spectra of the OLR and the OLR-based spheres are all similar. This result indicates that neither the variations in the ratio of the ethanol/water mixture nor the homogenization time had a distinct influence on the functional groups or basic structure of the OLR-based spheres.

The UV−vis spectra of the OLR-based spheres that regenerated from 50% ethanol/water solution contain three main absorption bands (Figure 6). The first one is located at 207 nm, corresponding to the E band of the $\pi-\pi^*$ transitions of the OLR. The second and third ones are located at 235 and 276 nm and are attributed to the B band of the $\pi-\pi^*$ transition of the aromatic groups.[24,26] There is essentially no change in these bands before and after homogenization, demonstrating that this processing has little effect on the chemical composition and bonding of the OLR and OLR-based spheres. According to the FTIR and UV−vis spectra, the characteristic peaks indicate that the functional groups and the chemical structure belonging to lignin remained unchanged when the homogenization time varied from 0 to 45 min and the ethanol content varied from 0 to 50%. The stability of the OLR structure laid the foundation for the formation of micellar submicron spheres.

To improve our understanding of the formation of the OLR-based colloidal spheres, possible mechanisms were investigated based on the above results. From the 2D HSQC NMR analysis, the ether bonds mostly disappeared, and the carbon-to-carbon bonds were richly distributed in the OLR, linking with a small amount of hemicelluloses. Therefore, the OLR with hydrophobic and hydrophilic moieties and having a 3D structure was considered as building blocks. Both the hydroxyl groups and

DOI: 10.1021/acsomega.7b00285
ACS Omega 2017, 2, 2858−2865

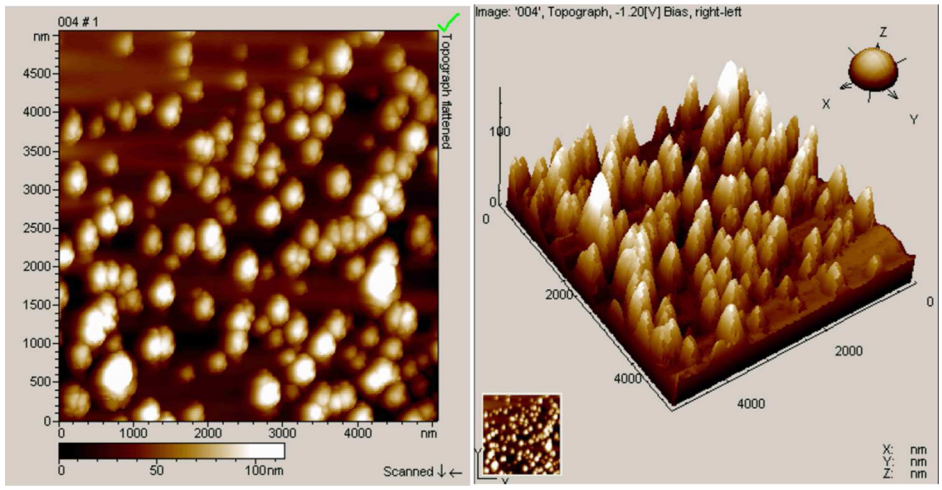

Figure 4. AFM images of the OLR-based submicron spheres regenerated from the ethanol/water solution (ethanol content: 50%), in conjunction with a 45 min homogenization.

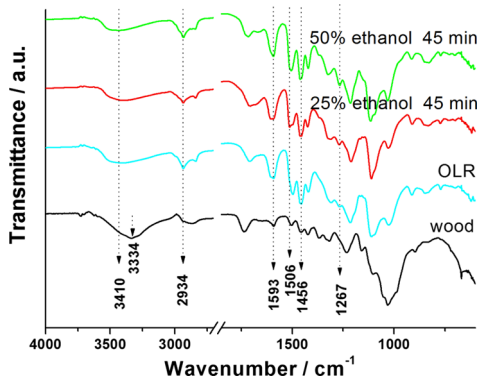

Figure 5. FTIR spectra of the wood, OLR, and OLR-based spheres generated from the ethanol/water solution (ethanol content: 25 and 50%, respectively), in conjunction with a 45 min homogenization.

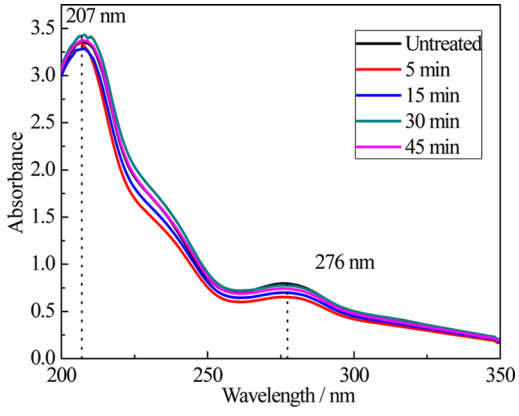

Figure 6. UV−vis spectroscopy of the OLR and OLR-based spheres generated from the ethanol/water solution (ethanol content: 50%), in conjunction with a homogenization for 5, 15, 30, and 45 min, respectively.

the newly formed carboxyl groups in the OLR molecules were expected to act as hydrophilic sites and distributed randomly in the complicated structure of OLR, whereas the aliphatic groups and aromatic skeletons were hydrophobic. When being added into the water/ethanol solution, the hydrophilic parts of the OLR molecules prompted their affinity to ethanol, whereas the hydrophobic parts of the OLR molecules promoted the formation of electrical double layers, forming the dispersion of stable spheres in the water/ethanol solution.[19,24] Thus, the hydrophobic regions tend to aggregate to form the yolks of the colloidal spheres, with the regenerated dissociation lignin parts forming the shells (Figure 7). This process is simultaneously facilitated by both van der Waals and $\pi-\pi$ interactions. The OLR aggregates are likely to form larger spheres or agglomeration when the ethanol content is insufficient to dissociate all hydrophobic parts, and the homogenization is not enough to destroy the intermolecular structure. If the ethanol content is high enough to dissociate most of the hydrophobic sections, then the OLR aggregates will not form cores and the balance between the hydrophilic and hydrophobic parts in solution will be disrupted. Therefore, to solve the agglomeration of the submicron lignin spheres, the ethanol content and the homogenizing time are improved to 50% and 45 min. In this case, the hydrophilic and hydrophobic parts facilitated by both van der Waals and $\pi-\pi$ interactions will form the shells and yolks of the colloidal spheres, respectively. Furthermore, the high shear force applied during homogenization can promote the formation of spheres at the same time, and the hydrophobic parts are compacted to produce submicron or smaller spheres. These OLR-based spheres exhibit high specific surface areas and good reactivity because of the destruction of interunit linkages and the generation of multiple functional groups. The OLR-based spheres show a significant potential as precursors that may have applications to energy storage, drug delivery, and templated syntheses.[18,27−31]

CONCLUSIONS

This study demonstrates an approach to fabricate the OLR-based spheres using differing ratios of ethanol/water combined with a homogenization process. The OLR extracted from the wood was found to contain amphiphilic portions and showed a higher solubility in ethanol than those of alkali lignin and kraft lignin. As a result, the hydrophobic parts of the material aggregated into spherical cores in the ethanol/water solution, whereas the hydrophilic regions formed shells through the van der Waals interactions of the aliphatic groups and the $\pi-\pi$ interactions of the aromatic groups. The morphology and the size of the OLR-based spheres were significantly affected by the ethanol content. The homogenization treatment was also found

DOI: 10.1021/acsomega.7b00285
ACS Omega 2017, 2, 2858−2865

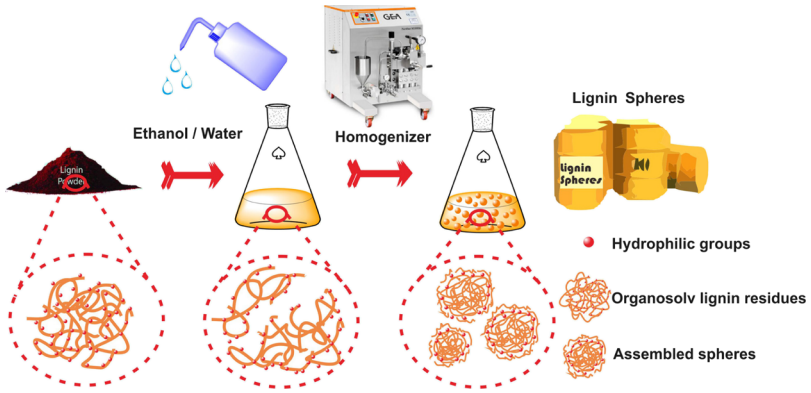

Figure 7. Schematic diagram shows the aggregation and regeneration of the OLR-based submicron spheres.

to facilitate the densification of the OLR assemblies through the application of a high shear force, and this processing had no effects on the stability of the chemical components or bonds in the OLR-based submicron spheres.

EXPERIMENTAL SECTION

Materials. Poplar wood (*Populus ussuriensis* Kom.) powder was used as a feedstock for the extraction of OLR. Ethanol, sulfuric acid, alkali lignin, and kraft lignin used in this work were of analytical grade and were purchased from the Kermel Chemical Reagent Co., Ltd. (Tianjin, China).

Extraction and Purification of OLR. The OLR was separated from the black liquor of the acid-catalyzed ethanol pulping of wood. In this process, a Teflon-lined stainless steel reactor (100 mL) was used as the experiment container. Poplar wood powder (6.0 g) was used as the raw material, and 75% (v/v) ethanol solution was employed as the solvent, with 0.12% (w/w, percentage of oven dry wood) H_2SO_4 added as a catalyst. The solid/liquid ratio in the reaction mixtures was 1:10 (g/mL), and each reaction was carried out at 180 °C over 80 min. The black liquor generated in the reactor was subsequently passed through a 0.45 μm filter, and the filtrate was collected. The solid residue was washed three times with an ethanol solution of 75% (v/v), and the washings were added to the filtrate. Finally, a volume of distilled water equal to three times the total filtrate volume was added to the filtrate to precipitate the OLR. The OLR was purified by an acid hydrolysis method. The OLR (0.3308 g) was added to 72% H_2SO_4 (5 mL) with vigorous stirring at room temperature for 2 h. Then, the suspension was diluted with distilled water to 3% sulfuric acid and refluxed continuously for 4 h. The purified organosolv lignin was separated by filtering and washed with distilled water.

Solubility of OLR, Kraft Lignin, and Alkali Lignin in Ethyl Alcohol. Excess amounts of OLR, alkali lignin, and kraft lignin were separately dispersed in 10 mL of ethanol and subjected to ultrasonication for 20 min. The mixtures were subsequently filtered through a 0.45 μm nylon membrane. The solubility of each material was calculated by determining the mass fraction of the saturated lignin solution.

Assembly of OLR into Spheres. A 0.3 g OLR sample was dissolved in 100 mL of the ethanol/water solution overnight, with magnetic stirring. According to the volume ratio of ethanol/water, the trials were divided into three groups that have different ethanol contents: 0% ethanol content, 25% ethanol content, 50% ethanol content, and 75% ethanol content. Typically, the OLR in the 50% ethanol solution was processed using a homogenizer (APV-2000, SPW Corp., Charlotte, USA) for 5, 15, 30, or 45 min. The homogenizer was set at an operating pressure of 100 bars for homogenizing valve 1 and 450 bars for homogenizing valve 2.

Characterization. *OLR Yield.* The Klason lignin yield was determined according to TAPPI Standards T 222 om-88,[20] and the OLR yield was expressed as the wt % of Klason lignin. Each sample was analyzed a minimum of three times, and the average values were reported.

$^1H-^{13}C$ Correlation 2D HSQC NMR Spectroscopy. In the preparation of NMR studies, a 90 mg sample of OLR was dissolved in 0.5 mL of deuterated dimethyl sulfoxide (DMSO-d_6). The 2D HSQC NMR spectra were recorded on an Agilent ProPulse 500 MHz spectrometer (Agilent Tech., Santa Clara, USA) and recorded in the gradient HSQC adiabatic mode. The spectral widths were 20 000 and 5000 Hz for the ^{13}C and ^1H dimensions, respectively. A total of 1024 complex points were collected for the ^1H dimension, with a recycle delay of 1.5 s and 128 transients, whereas 256 time increments were recorded in the ^{13}C dimension. Before Fourier transformation, the data matrices were zero-filled to 1024 points in the ^{13}C dimension.

GPC Analysis. A 0.4 g OLR or the OLR after homogenization for 45 min was acetylated in 10 mL of an acetylation reagent (consisting of 23.48 mL of acetic anhydride, 20.24 mL of pyridine, and 21.3 mL of dioxane) to improve the solubility of the lignin in THF. The molecular weight of the lignin was subsequently ascertained based on GPC using an Agilent 1100 high-performance liquid chromatograph (Agilent Tech., Wilmington, USA) equipped with a HP 1100 variable wavelength detector and a 2128 fraction collector (Bio-Rad, Hercules, CA, USA), employing THF as the eluant at 1.0 mL min^{-1}. Polystyrene was employed as the standard substance to calibrate the instrument.

FTIR Spectroscopy. FTIR spectra were recorded using a Nicolet 6700 (Thermo Fisher Scientific Inc., Waltham, USA) in the attenuated total reflectance (ATR) mode, from 600 to 4000 cm^{-1} with a resolution of 4 cm^{-1}.

UV–Vis Spectroscopy. A Cary 100 spectrometer (Varian, Mulgrave, Australia) was utilized to determine the functional groups of the OLR in the ethanol/water solution before and after homogenization, over the wavelength range of 190–800 nm. The OLR concentration in these samples was approximately 0.3% (w/w).

TEM Observations. TEM observations were made using a JEM-2100 microscope (JEOL, Tokyo, Japan) at an accelerating voltage of 200 kV. The samples in solution were first dropped

DOI: 10.1021/acsomega.7b00285
ACS Omega 2017, 2, 2858–2865

onto a copper grid coated with a carbon film and then air-dried for 3 min to allow ethanol and water to evaporate.

AFM Analyses. AFM observations were made with a Pico Plus instrument (Agilent Tech., Tempe, USA). The AFM samples were prepared by slowly dispersing the OLR spherical colloids on a quartz slide, followed by drying at room temperature for 24 h.

■ ASSOCIATED CONTENT

Supporting Information

The Supporting Information is available free of charge on the ACS Publications website at DOI: 10.1021/acsomega.7b00285.

Figures for 2D HSQC NMR characterization of MWL and the panoramic TEM photos of the OLR-based submicron spheres (PDF)

■ AUTHOR INFORMATION

Corresponding Author

*E-mail: yuhaipeng20000@gmail.com (H.Y.).

ORCID

Haipeng Yu: 0000-0003-0634-7913

Notes

The authors declare no competing financial interest.

■ ACKNOWLEDGMENTS

This work was supported by the National Natural Science Foundation of China (grant no. 31622016) and the Natural Science Foundation of Heilongjiang Province of China (grant no. JC2016002).

■ REFERENCES

(1) Whetten, R.; Sederoff, R. Lignin Biosynthesis. *Plant Cell* **1995**, *7*, 1001−1013.

(2) Boerjan, W.; Ralph, J.; Baucher, M. Lignin Biosynthesis. *Annu. Rev. Plant Biol.* **2003**, *54*, 519−546.

(3) Jiang, C.; He, H.; Jiang, H.; Ma, L.; Jia, D. M. Nano-Lignin Filled Natural Rubber Composites: Preparation and Characterization. *eXPRESS Polym. Lett.* **2013**, *7*, 480−493.

(4) Tran, C. D.; Chen, J.; Keum, J. K.; Naskar, A. K. A New Class of Renewable Thermoplastics with Extraordinary Performance from Nanostructured Lignin-Elastomers. *Adv. Funct. Mater.* **2016**, *26*, 2677−2685.

(5) Laurichesse, S.; Avérous, L. Chemical Modification of Lignins: Towards Biobased Polymers. *Prog. Polym. Sci.* **2014**, *39*, 1266−1290.

(6) Zhang, Y.-H. P. Reviving the Carbohydrate Economy via Multi-Product Lignocellulose Biorefineries. *J. Ind. Microbiol. Biotechnol.* **2008**, *35*, 367−375.

(7) Qian, Y.; Qiu, X.; Zhu, S. Lignin: A Nature-Inspired Sun Blocker for Broad-Spectrum Sunscreens. *Green Chem.* **2015**, *17*, 320−324.

(8) Ksibi, M.; Amor, S. B.; Cherif, S.; Elaloui, E.; Houas, A.; Elaloui, M. Photodegradation of Lignin from Black Liquor Using a UV/TiO_2 System. *J. Photochem. Photobiol., A* **2003**, *154*, 211−218.

(9) Ragauskas, A. J.; Beckham, G. T.; Biddy, M. J.; Chandra, R.; Chen, F.; Davis, M. F.; Davison, B. H.; Dixon, R. A.; Gilna, P.; Keller, M.; Langan, P.; Naskar, A. K.; Saddler, J. N.; Tschaplinski, T. J.; Tuskan, G. A.; Wyman, C. E. Lignin Valorization: Improving Lignin Processing in the Biorefinery. *Science* **2014**, *344*, 1246843.

(10) Kubo, S.; Kadla, J. F. The Formation of Strong Intermolecular Interactions in Immiscible Blends of Poly(vinyl alcohol) (PVA) and Lignin. *Biomacromolecules* **2003**, *4*, 561−567.

(11) Nair, S. S.; Sharma, S.; Pu, Y.; Sun, Q.; Pan, S.; Zhu, J. Y.; Deng, Y.; Ragauskas, A. J. High Shear Homogenization of Lignin to Nanolignin and Thermal Stability of Nanolignin-Polyvinyl Alcohol Blends. *ChemSusChem* **2014**, *7*, 3513−3520.

(12) Tortora, M.; Cavalieri, F.; Mosesso, P.; Ciaffardini, F.; Melone, F.; Crestini, C. Ultrasound Driven Assembly of Lignin into Microcapsules for Storage and Delivery of Hydrophobic Molecules. *Biomacromolecules* **2014**, *15*, 1634−1643.

(13) Qian, Y.; Deng, Y.; Qiu, X.; Li, H.; Yang, D. Formation of Uniform Colloidal Spheres from Lignin, A Renewable Resource Recovered from Pulping Spent Liquor. *Green Chem.* **2014**, *16*, 2156−2163.

(14) Argyropoulos, D. S.; Crestini, C. A Perspective on Lignin Refining, Functionalization, and Utilization. *ACS Sustainable Chem. Eng.* **2016**, *4*, 5089.

(15) Gilca, I. A.; Ghitescu, R. E.; Puitel, A. C.; Popa, V. I. Preparation of Lignin Nanoparticles by Chemical Modification. *Iran. Polym. J.* **2014**, *23*, 355−363.

(16) Lievonen, M.; Valle-Delgado, J. J.; Mattinen, M.-L.; Hult, E.-L.; Lintinen, K.; Kostiainen, M. A.; Paananen, A.; Szilvay, G. R.; Setälä, H.; Österberg, M. A Simple Process for Lignin Nanoparticle Preparation. *Green Chem.* **2016**, *18*, 1416−1422.

(17) Frangville, C.; Rutkevičius, M.; Richter, A. P.; Velev, O. D.; Stoyanov, S. D.; Paunov, V. N. Fabrication of Environmentally Biodegradable Lignin Nanoparticles. *ChemPhysChem* **2012**, *13*, 4235−4243.

(18) Deng, Y.; Feng, X.; Zhou, M.; Qian, Y.; Yu, H.; Qiu, X. Investigation of Aggregation and Assembly of Alkali Lignin using Iodine as a Probe. *Biomacromolecules* **2011**, *12*, 1116−1125.

(19) Li, H.; Deng, Y.; Liu, B.; Ren, Y.; Liang, J.; Qian, Y.; Qiu, X.; Li, C.; Zheng, D. Preparation of Nanocapsules via the Self-Assembly of Kraft Lignin: a Totally Green Process with Renewable Resources. *ACS Sustainable Chem. Eng.* **2016**, *4*, 1946−1953.

(20) TAPPI Standards T 222 om-88. Acid-Insoluble Lignin in Wood and Pulp. In *TAPPI Test Methods*, 1999.

(21) Chen, W.; Yu, H.; Liu, Y.; Hai, Y.; Zhang, M.; Chen, P. Isolation and Characterization of Cellulose Nanofibers from Four Plant Cellulose Fibers Using a Chemical-Ultrasonic Process. *Cellulose* **2011**, *18*, 433−442.

(22) Capanema, E. A.; Balakshin, M. Y.; Kadla, J. F. A Comprehensive Approach for Quantitative Lignin Characterization by NMR Spectroscopy. *J. Agric. Food Chem.* **2004**, *52*, 1850−1860.

(23) Liu, Y.; Chen, W.; Xia, Q.; Guo, B.; Wang, Q.; Liu, S.; Liu, Y.; Li, J.; Yu, H. Efficient Cleavage of Lignin-Carbohydrate Complexes and Ultrafast Extraction of Lignin Oligomers from Wood Biomass by Microwave-Assisted Treatment with Deep Eutectic Solvent. *ChemSusChem* **2017**, *10*, 1692−1700.

(24) Xiong, F.; Han, Y.; Wang, S.; Li, G.; Qin, T.; Chen, Y.; Chu, F. Preparation and Formation Mechanism of Size-Controlled Lignin Nanospheres by Self-Assembly. *Ind. Crops Prod.* **2017**, *100*, 146−152.

(25) Li, Y.; Liu, Y.; Chen, W.; Wang, Q.; Liu, Y.; Li, J.; Yu, H. Facile Extraction of Cellulose Nanocrystals from Wood using Ethanol and Peroxide Solvothermal Pretreatment Followed by Ultrasonic Nanofibrillation. *Green Chem.* **2016**, *18*, 1010−1018.

(26) Ouyang, X.; Deng, Y.; Qian, Y.; Zhang, P.; Qiu, X. Adsorption Characteristics Of Lignosulfonates in Salt-Free and Salt-Added Aqueous Solutions. *Biomacromolecules* **2011**, *12*, 3313−3320.

(27) Alvarez-Vasco, C.; Ma, R.; Quintero, M.; Guo, M.; Geleynse, S.; Ramasamy, K. K.; Wolcott, M.; Zhang, X. Unique Low-Molecular-Weight Lignin with High Purity Extracted from Wood by Deep Eutectic Solvents (DES): A Source of Lignin for Valorization. *Green Chem.* **2016**, *18*, 5133−5141.

(28) Ago, M.; Huan, S.; Borghei, M.; Raula, J.; Kauppinen, E. I.; Rojas, O. J. High-Throughput Synthesis of Lignin Particles (~30 nm to ~2 μm) via Aerosol Flow Reactor: Size Fractionation and Utilization in Pickering Emulsions. *ACS Appl. Mater. Interfaces* **2016**, *8*, 23302−23310.

(29) Jeon, J.-W.; Zhang, L.; Lutkenhaus, J. L.; Laskar, D. D.; Lemmon, J. P.; Choi, D.; Nandasiri, M. I.; Hashmi, A.; Xu, J.; Motkuri, R. K.; Fernandez, C. A.; Liu, J.; Tucker, M. P.; McGrail, P. B.; Yang, B.; Nune, S. K. Controlling Porosity in Lignin-Derived Nanoporous Carbon for Supercapacitor Applications. *ChemSusChem* **2015**, *8*, 428−432.

DOI: 10.1021/acsomega.7b00285
ACS Omega 2017, 2, 2858−2865

(30) Zhao, D.; Zhang, Q.; Chen, W.; Yi, X.; Liu, S.; Wang, Q.; Liu, Y.; Li, J.; Li, X.; Yu, H. Highly Flexible and Conductive Cellulose-Mediated PEDOT:PSS/MWCNT Composite Films for Supercapacitor Electrodes. *ACS Appl. Mater. Interfaces* **2017**, *9*, 13213−13222.
(31) Zhao, D.; Chen, C.; Zhang, Q.; Chen, W.; Liu, S.; Wang, Q.; Liu, Y.; Li, J.; Yu, H. High Performance, Flexible, Solid-State Supercapacitors Based on a Renewable and Biodegradable Mesoporous Cellulose Membrane. *Adv. Energy Mater.* **2017**, *7*, 1700739.

DOI: 10.1021/acsomega.7b00285
ACS Omega 2017, 2, 2858−2865